

TABLE 1
INFLUENCE OF NEUTRON IRRADIATION ON SELECTIVITY OF γ - Al_2O_3

Pretreatment temperature (°C)	Total flux n.v.t.	Number type A/m ²	Number type B/m ²	Total (A + B)/m ²	% <i>trans</i> conversion per A site
500	—	1.1×10^{17}	0.3×10^{17}	1.4×10^{17}	0.34×10^{-17}
500	10^{17}	1.3×10^{17}	0.1×10^{17}	1.4×10^{17}	0.27×10^{-17}
700	—	0.95×10^{17}	0.4×10^{17}	1.3×10^{17}	0.37×10^{-17}
700	10^{17}	1.1×10^{17}	0.2×10^{17}	1.3×10^{17}	0.29×10^{-17}

between curves for activity and amount of sites are only of a rough nature. The activity values for the formation of c.b-2 show a stronger increase in the preheating temperature range between 400° and 600°C than the total amount of sites, indicating that the activity per site increases. This coincides with an increase in acid strength of the active centers as has been found by MacIver (2). Above 600°C the activity per site and acid strength (MacIver) decreases. Reasons for both changes in amount and acidity of active sites should be sought in structural changes caused by the heat treatment. Dehydration of the surface at lower temperatures (400–600°C) leads to a decrease of hydroxyl groups and an increase of aluminum atoms in the surface involving a conversion of type B to type A sites. At higher temperatures (>650°C) both types diminish in amount because of recrystallization processes in the surface.

As is shown in Table 1 the conversion of type B to type A sites can also be promoted by neutron irradiation even in a catalyst which was already submitted to a heat treatment by which a nearly optimal formation of type A sites was obtained. Obviously this leads to an increase in total

activity (Fig. 2). However, it was found (compare last column in Table 1) that the activity per A site decreases at the same time. Though the irradiation was done with a mixture of slow and fast neutrons in combination with γ radiation it seems most plausible that fast neutrons are responsible for knocking out more oxygen atoms and hydroxyl groups from the surface. The resulting increase of type A sites leads to a higher activity for t.b-2 formation and to an extremely low value for the *cis/trans* ratio. The latter is not changed any more at higher radiation dose, indicating that an equilibrium mixture of the two active sites has been formed.

REFERENCES

1. MEDEMA, J., AND HOUTMAN, J. P. W., *J. Catalysis* **6**, 322 (1966) (preceding paper).
2. MACIVER, D. S., TOBIN, H. H., AND BARTH, R. T., *J. Catalysis* **2**, 485 (1963).

J. MEDEMA
J. P. W. HOUTMAN

Reactor Instituut at Delft
The Netherlands
Received June 15, 1966

Surface Properties of Nickel Oxide

The qualitative electronic theory of catalysis, as developed by Volkenstein (1), predicts that the position of the Fermi level of a semiconducting catalyst and also its adsorptive capacity depend upon the

particle or crystallite size below a certain critical dimension. This Note reports the results of electrical measurements on a series of small particles of NiO and the effect of adsorbed water on these properties.

Nickel oxide samples were prepared by heating nickel hydroxide in air or nitrogen over the temperature range 250°–1000°C (2). Particle sizes, measured by electron diffraction line broadening, varied from 73 to $>10^4$ Å. Surface areas were measured by the nitrogen BET method. Bunsen-Rupp tests showed the samples to be Ni_{1-x}O with x ranging from 0.017 to almost zero as the temperature of heat-treatment increased. This dependence has been well substantiated by others (2–5) but is at variance with Mitoff (6), who found that x increased above 600°C with increasing temperature and oxygen pressure. Mitoff's measurements reflect equilibrium conditions of pure NiO at very high temperatures, whereas the nonstoichiometry reported here results from the decomposition of the initial hydroxide without equilibrium with the atmosphere.

Seebeck coefficients were measured in a ceramic holder designed to clamp a small pill (1×0.3 cm in diameter) between platinum electrodes. A small heater and appropriate thermocouples were provided to establish and measure a thermal gradient of 5° across the sample pill. The thermocouple differences and the thermal emf were measured with a Leeds and Northrup K-3 potentiometer. Resistance measurements were made with an impedance bridge. The apparatus was positioned in a vacuum manifold so that readings before and after evacuation could be made. The vacuum manifold also contained a quartz spring balance (sensitivity 1.045 mg/mm), thus providing for simultaneous weight loss measurements on aliquot portions of the sample under investigation.

After preparation, the samples were stored in a constant humidity atmosphere (15 mm H_2O vapor pressure) until used. Each sample was pill and loaded into the apparatus. At the same time a sample for weight loss measurement was prepared. Measurements of the Seebeck effect, QT , and conductivity, σ , were made at room temperature in air. The system was then evacuated and the weight of the sample followed until constant. The values QT and σ were again measured. In a separate experiment, the material evacuated from the

sample was trapped and found to be water. The measurements were reversible, the original QT value returning when the pill was exposed to the constant humidity atmosphere.

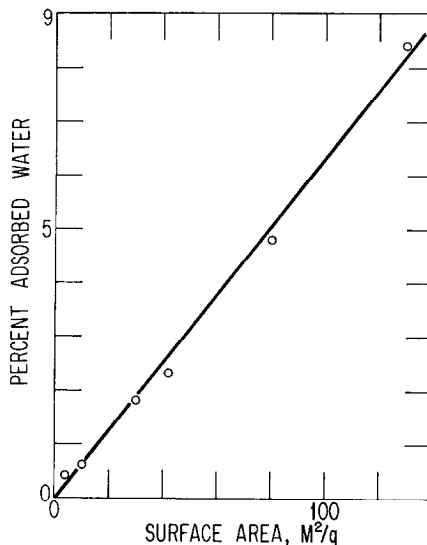


Fig. 1. Percent water adsorbed versus surface area for NiO samples.

Figure 1 shows the weight percent water plotted against nitrogen surface area. A value of 2.12×10^{15} molecules/cm² was determined for the value of N , the concentration of adsorbed molecules. Figure 2

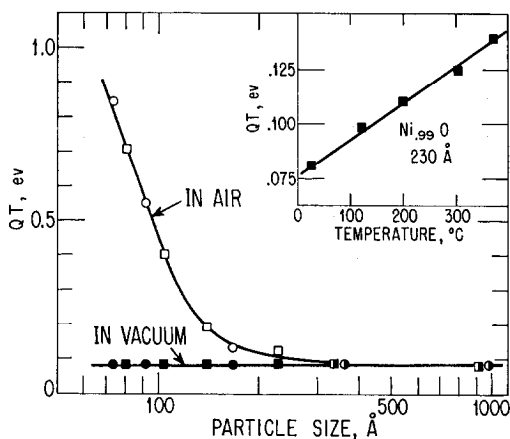


Fig. 2. Seebeck effect, QT , at 25°C versus particle size for NiO. The insert shows the temperature dependence for one of the samples. □ Heat-treated in N_2 ; ○ Heat-treated in air.

gives the value of QT at 25°C before and after evacuation, as a function of particle size. Below 350 Å, the effect of the adsorbed water on QT increases as the particle size decreases. The insert shows the temperature dependence for QT of the 230 Å sample after evacuation. There is no large effect due to heat-treatment in air or nitrogen. Figure 3 shows the conductivity as a func-

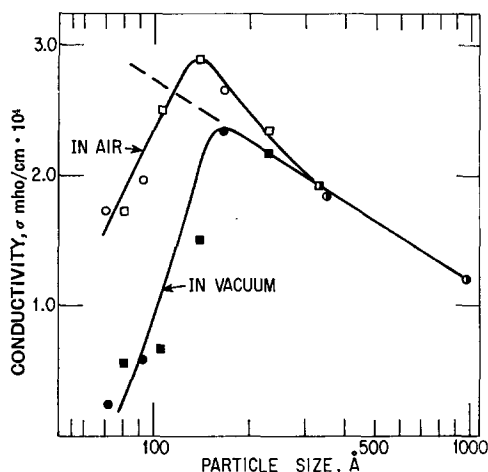


Fig. 3. Conductivity versus particle size.

tion of particle size. The conductivity values were independent of frequency up to 10^6 cps.

The semiconducting properties of NiO have been explained (7-9) by the conduction mechanism of d holes "jumping" from Ni^{3+} to Ni^{2+} sites. For stoichiometric NiO this involves excitation of electrons from filled Ni^{2+} levels (E_0) to empty Ni^+ levels (E_1). This intrinsic energy is large so that pure NiO is an insulator. However, for $Ni_{1-x}O$, $2x$ acceptor levels (E_a) are created above the Ni^{2+} levels, thus creating Ni^{3+} sites for the conduction. Since conduction is by 3d holes, the Fermi level, E_F , is given by

$$E_F = QT + E_0 \quad (1)$$

After the treatment for $Li_xNi_{(1-x)}O$ (9),

$$QT = 1/2kT \ln (1/2x) + 1/2(E_a - E_0) \quad (2)$$

describes the data given in the insert of Fig. 2. The value of $(E_a - E_0)$ was found to be 0.056 eV for $x = 0.010$.

Volkenstein (1) considers the case of a

semiconducting adsorbent whose dimensions are less than the depth of the space charge and concludes that the position of the Fermi level of small particles is the same in the bulk material and at the surface. Furthermore, he derives a relationship between the Fermi level and particle size for particles well below the dimensions of the space charge region and containing charged adsorbed species. In NiO, the space charge is established by the mobile holes in the p -band rather than by the localized charges in the d -band. Under these conditions the depth of the space charge region, l , is then

$$l = \left[\frac{\Sigma kT}{2\pi q^2 N_c \exp(-E_F/kT)} \right]^{1/2}, \quad (3)$$

where Σ = dielectric constant

where q = electronic charge

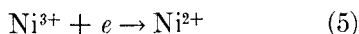
where N_c = density of states.

The dielectric constant for NiO has been reported as 12 (10). By using this number instead of the value of 5 assumed by Morin (8) in his theoretical calculation of the band picture, the position of the 3d levels, E_0 , is 0.125 eV above the 2p band. The data in Fig. 2 show that the largest particles have a QT of 0.080 eV, placing the Fermi level 0.205 eV above the 2p band. The value of N_c at 300°K is $2.4 \times 10^{19} \text{ cm}^{-3}$, so that from Eq. (3)

$$l = 635 \text{ Å}$$

This is remarkably good agreement with Parravano's (11) experimental estimate of 600 Å. The results in Fig. 2 tend to substantiate qualitatively Volkenstein's theory that for particles less than the size of the space charge depth, the Fermi level of the adsorbent will depend upon the dimensions. However, it is not possible from these data alone to verify the quantitative expressions given, since QT increases much faster than predicted.

Parravano and Domenicalli (11) have discussed the thermoelectric properties of small particles and have concluded that the value QT should reflect directly electron transfer effects associated with chemisorption. Thus, for water adsorption, only the process



would result in a decrease in the Ni^{3+} concentration and a resulting increase in E_f and QT . If the fraction of adsorbed molecules in the charged state did not change too much, the effect of these surface electrons would be expected to increase inversely with particle size. Accordingly, QT would increase as the crystal dimension decreases. However, in this event, chemisorption of H_2O on the smallest particles should result in a change of Ni^{3+} concentration by a factor of 10^{-13} , with a corresponding decrease in conductivity. Figure 3 shows that this is not the case. Neither the model of Volkenstein nor that of Parravano completely explain the observations, i.e., decreasing the particle size of the absorbent gives an increasing value of QT but also an increasing hole conductivity with adsorption.

The results may be understood, however, if the energy band structure for NiO is modified to include H_2O^+ levels. Figure 4

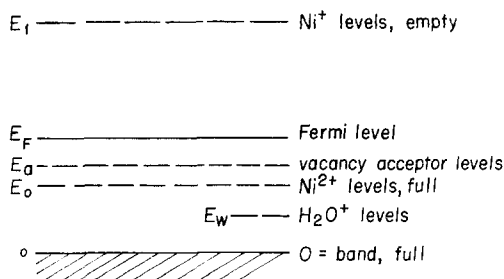


FIG. 4. Energy band scheme for small particles for NiO , including levels for adsorbed water.

shows the energy level scheme. The small size of the particles results in a model where bulk and surface are essentially the same and both respond to changes (1). For a material without charged surface species, the conductive mechanism occurs via the hole jumping from Ni^{3+} to Ni^{2+} and is proportional to Ni^{3+} concentration. The Fermi level and QT are essentially constant with particle size since x does not change drastically below 1000 \AA . As H_2O adsorption

takes place, two processes occur. Part of the water molecules are charged according to (4). This results in a decrease in Ni^{3+} concentration with a corresponding increase in E_F and decrease in σ .^{*} At the same time, the H_2O^+ species produce impurity levels situated at E_w , between the Ni^{2+} levels and the O^{2-} band. The location of these levels is situated consistent with Eqs. (3) and (4) of this model. However, there is some physicochemical justification for this choice in the calculations of Dowden (12) who estimated the ionization energies of the Ni^{2+} in $\text{Ni}-\text{H}_2\text{O}$ and $\text{Ni}-\text{O}$ bonds to be 9.0 and 8.0 eV, respectively. Accordingly, H_2O molecules adsorbed on the NiO surface could form a co-ordinated chemisorption bond with exposed Ni^{2+} ions, through the $3d$ orbitals. This bond constitutes the donor level, E_w , which, with the usual dielectric correction, would be located approximately 0.083 eV below E_o .

Charged H_2O^+ surface states have been detected on silicon and germanium surfaces (13, 14). Eriksen *et al.* (14) have shown that, for a sufficiently thick water film (about 10 monolayers) on germanium, an excess surface current occurs that may be attributed to the "hole" conduction of electrons hopping from H_2O^+ species to the neutral chemisorbed H_2O molecules existing in the first monolayer. This conductivity has a mobility of $1-50 \text{ cm}^2/\text{V sec}$. The water film on the NiO surfaces is about 2 to 3 layers thick, so that a similar excess surface conduction could occur by "hopping" from H_2O^+ levels or even within a narrow H_2O^+ band. This would result in a surface conduction Σ_w and a Seebeck effect given by

$$(QT)\sigma = (E_F - E_o)\sigma_h + (E_f - E_w)\frac{\Sigma_w}{L}, \quad (6)$$

where L is the crystal size, σ_h the conductivity due to the Ni^{3+} ions. Also,

^{*} It is possible that the decrease in conductivity of the evacuated samples below 150 \AA may be attributed to this effect, since it is probable that some water molecules remain on the surface even after the evacuation. These residual molecules could supply enough electrons to account for the decrease in conductivity but not enough to greatly alter the Fermi level.

$$\sigma = \sigma_h + \frac{\Sigma \omega}{L} \quad (7)$$

With $(E_t - E_\omega)$ large enough, adsorption will result in an increase of QT that varies inversely with particle size. Furthermore, an increase in σ is possible according to (6) if the surface conductance is large enough to overcome the decrease in conductivity of Ni^{3+} holes.

This model qualitatively accounts for the observations. Similar effects should be detected with films produced by other condensable vapors such as acetone and alcohols. However, further analysis of these parameters is complicated by the many processes involved. It is clear that the over-all electrical properties of a semi-conducting catalyst, prepared in the particle size range of interest in practice, are functions of the charged adsorbed species and the particle size. Theories of catalysis that attempt to reconcile surface electrical properties and catalytic mechanisms with measured quantities must take the above factors into account.

REFERENCES

1. VOLKENSTEIN, T., *Advan. Catalysis* **12** (1960).
2. RICHARDSON, J. T., AND MILLIGAN, W. O., *Phys. Rev.* **102**, 1289 (1956).

3. DEREN, J., HABER, J., AND STOCZYNSKI, J., *Bull. Acad. Pol. Sci. Ser. Sci. Chim.* **9**, 245 (1961).
4. KUTSEVA, L. N., *Dokl. Akad. Nauk SSSR* **138**, 409 (1961).
5. YOSHIO, I., SHIMADO, K., AND OZAKI, S., *J. Chem. Soc. Japan* **33**, 1372 (1960).
6. MITOFF, S. P., *J. Chem. Phys.* **35**, 882 (1961).
7. DE BOER, J. H., AND VERWEY, E. J. W., *Proc. Phys. Soc. London* **49**, 59 (1937).
8. MORIN, F. J., *Bell. Syst. Tech. J.* **37**, 1047 (1958).
9. VAN HOUTEN, S., *J. Phys. Chem. Solids* **17**, 7 (1960).
10. RAO, K. V., AND SMAKULA, A., *J. Appl. Phys.* **36**, 2031 (1965).
11. PARRAVANO, G., AND DOMENICALLI, C. A., *J. Chem. Phys.* **26**, 359 (1957).
12. DOWDEN, D. A., AND WELLS, D., *Actes du Deuxieme Congrès International de Catalyse*, p. 1499, Editions Technip, Paris (1961).
13. JÄNTSCH, O., *J. Phys. Chem. Solids* **26**, 1233 (1965).
14. ERIKSEN, W. T., STATZ, H., AND DE MARS, G. A., *J. Appl. Phys.* **28**, 133 (1957).

JAMES T. RICHARDSON

*Esso Research and Engineering Company
Baytown Research and Development Division
Baytown, Texas*

Received July 16, 1965;

revised June 17, 1966

X-Ray Studies of a Bismuth Molybdate Catalyst under Reaction Conditions

Studies designed to correlate activity and selectivity with catalyst composition or structure represent an attempt to elucidate the way in which the catalyst functions. Central to these studies is a determination of the structure of the catalytically active phase. In the past, the great majority of catalyst structure studies have been performed under conditions substantially removed from reaction conditions. A question immediately arises as to the resemblance, if any, between the structure existing under

these conditions convenient for physical measurements and the structure existing under actual catalytic reaction conditions. This question, while asked before by others, rarely has been subjected to systematic study. An X-ray study by Isaev and Kushnerev (1) on a copper oxide catalyst is one of the few performed under reaction conditions.

The purpose of this note is to present XRD data obtained on an active bismuth molybdate catalyst in the conventional